

See discussions, stats, and author profiles for this publication at: <https://www.researchgate.net/publication/230251872>

Microphase separation in poor-solvent polyelectrolyte solutions: Phase diagram

ARTICLE *in* MACROMOLECULAR THEORY AND SIMULATIONS · JULY 1994

Impact Factor: 1.67 · DOI: 10.1002/mats.1994.040030403

CITATIONS

22

READS

17

3 AUTHORS, INCLUDING:



Igor Erukhimovich

Lomonosov Moscow State University

100 PUBLICATIONS 1,432 CITATIONS

SEE PROFILE

Microphase separation in poor-solvent polyelectrolyte solutions: phase diagram

*Elena E. Dormidontova, Igor Ya. Erukhimovich^{a)}, Alexei R. Khokhlov**

Physics Department, Moscow State University, Moscow 117234, Russia

(Received: October 15, 1993; revised manuscript of February 8, 1994)

SUMMARY:

Microphase separation in solutions of weakly charged polyelectrolytes in poor solvents is studied in the weak segregation limit within the framework of the mean field approximation using a method first developed by Leibler. As a result a complete phase diagram of the solution near the critical point is obtained. The regions of stability of the disordered, homogeneous phase and of body-centered cubic (bcc), triangular and lamellar microdomain structures, as well as the phase separation regions are determined. The most striking difference in comparison with the corresponding diagram for block-copolymer melts is the existence of broad phase separation regions even for monodisperse systems. As the quality of solvent becomes poorer, the triangular microdomain structure remains the most stable among microdomain phases of other symmetry.

Introduction

The problem of microphase separation in polymer systems was attracting considerable attention in recent years. In particular, it was discovered that — in addition to block-copolymers^{1–5)} — this phenomenon can take place in many other polymer systems: random copolymers^{6–9)}, interpenetrating polymer networks^{10, 11)}, systems containing weakly charged polyelectrolytes^{12–18)}, ionomers¹⁹⁾ and in polymer mixtures with nonlocal entropy of mixing²⁰⁾. Thus, the concept of microphase separation has a much wider application in polymer physics than it was previously thought.

The specific physical reasons which lead to the formation of thermodynamically stable microdomain structures may be different. However, there is a common feature for each of the above-mentioned examples: namely, the interplay between the short-range immiscibility tendency and the opposite larger-range stabilizing factor which prevents the macroscopic demixing of the polymer system. For example, this stabilizing factor may be due to the connectivity of the blocks in one chain (for block-copolymers) or due to the contribution of mobile counterions to the entropy of mixing (for polyelectrolytes).

This fact leads to a remarkable similarity in the theoretical description of microphase separation in various polymer systems. In particular, the methods that were first developed for block-copolymer solutions and melts (the systems studied in most details) were afterwards fruitfully applied to newly discovered examples of microphase separation (cf. refs.^{6–20)}). The present paper is of the same style: the phase diagram for solutions of weakly charged polyelectrolytes in poor solvents near the critical point will be studied using the methods previously developed for block-copolymers.

^{a)} Also at Enterprise “Sitesoft”, 32, Kornejchuka str. 3, Moscow 127543, Russia.

The conclusion that microphase separation is possible for poor solvent solutions of weakly charged polyelectrolytes was first made in ref.¹²⁾ If polyelectrolyte macromolecules are only slightly charged there is a tendency towards polymer-solvent demixing for solvents which are poor with respect to the noncharged links. However, the separation of the solution into two macroscopic phases (dilute and concentrated) leads to a significant loss of translational entropy of the counter ions^{12–15, 21)}. Thus, in some situations a microdomain structure is the best choice from the point of view of the free energy.

This problem was further studied in refs.¹³⁾ and¹⁴⁾. Borue and Erukhimovich¹³⁾ have performed a detailed analysis of the behavior of polyelectrolyte solutions. They have obtained a phase diagram containing the microphase separation region. However, in the expression for the free energy they have not taken into account some factors which play an important role for determination of the conditions of stability and the physical properties of microdomain (supercrystal) phases (see below). Namely, the contribution to the free energy due to the translational entropy of solvent molecules was only partially (in the second-order terms) taken into account. Besides, the problem of macrophase separation and coexistence of phases having different supercrystal symmetries was not considered in ref.¹³⁾ at all. The aim of the present paper is to overcome these shortcomings; this will allow us to investigate not only microphases themselves, but also transitions between the phases of different symmetry, and to determine the full phase diagram near the critical point.

In ref.¹⁴⁾ Joanny and Leibler have investigated the possible structure of spherical micelles for poor enough solvents. On the basis of the analysis of the monomer-monomer correlation function they have obtained the same equation for the spinodal of microphase separation and the same expression for the period of microstructure as in ref.¹³⁾ They have not considered higher-order terms of expansion of the free energy and have not obtained the phase diagram.

For similar block-copolymer problems the corresponding calculations were performed long time ago. There are two main methods in studying this problem that complement each other. To study phase equilibria near the critical point it is convenient to use the expansion of the free energy in the powers of deviation of concentration of monomeric units from the homogeneous one. This approach (weak crystallization theory) is applied to weakly segregated systems. In polymer science it was first developed in ref.³⁾ (see also refs.^{4, 22)}). Another method, which can be applied to the well-formed microdomain structure with narrow interphases between the domains (strong segregation approximation), was developed in refs.^{5, 23, 24)} In the present paper we will calculate the phase diagram of polyelectrolyte solutions in a poor solvent within the framework of the weak crystallization theory.

This problem is now rather actual, since after the first theoretical predictions of the possibility of microphase separation in polyelectrolyte solutions^{12–15)} some experimental studies aimed to observe a microdomain structure in these system were reported in the literature^{25–27)}. In particular, the authors of ref.²⁷⁾ definitely claim that they have detected a microphase separation for polyelectrolyte gels in poor solvents (the gels are crosslinked while the solutions are not, however this difference is not of primary importance for the possible existence of microdomain structures). For further

experimental investigations in these directions it is, of course, worth-while to know theoretical predictions for the full phase diagram.

The further structure of this paper is organized as follows. In the next section we present the expression for the free energy of weakly charged polyelectrolyte solutions and obtain the equation for spinodal curves and the critical wave vector. Then we reduce the free energy to the form that is similar to the weak segregation approximation expansion as obtained by Leibler. The free energies for different microstructures are compared. Finally, we analyze the results and construct the phase diagrams for polyelectrolyte solutions.

Free energy of weakly charged polyelectrolyte solutions

Let us consider a solution of weakly charged polyelectrolytes. Let us assume that each weakly charged polymer chain is flexible and contains N monomer units; the fraction f ($f \ll 1$) of these units is positively charged with elementary charge $+e$. In addition, oppositely charged counterions are present in the solution to ensure its total electro-neutrality; we will assume that the solution is salt-free. For the description of the interactions in the polymer solution we will use the Flory-Huggins lattice model with the size of a cell b and the Flory-Huggins parameter of interaction between monomer units χ . Let $\Phi(r)$ be the volume fraction of polymer at the point r and $n(r)$ the concentration of counterions at this point. Then, within the framework of the self-consistent field approximation, we can write the free energy of the solution in the following form (cf. refs.^{17, 18)}

$$\frac{F}{kT} = \frac{I}{b^3} \int d^3r \left\{ \frac{\Phi}{N} \ln \Phi + (1 - \Phi) \ln (1 - \Phi) + nb^3 \ln (nb^3) \right. \\ \left. + \chi \Phi \cdot (1 - \Phi) + \frac{a^2}{24} \frac{(\nabla \Phi)^2}{\Phi} + \frac{1}{2} \frac{e}{kT} \phi \cdot (\Phi f - nb^3) \right\} \quad (1)$$

where T is the temperature, k the Boltzmann constant, $\phi(r)$ is the electrostatic potential at the point r and a the Kuhn segment length of an (uncharged) polymer chain. The calculations presented below for the sake of simplicity are performed for the case $a = b$ which corresponds to flexible polymer chains. The electrostatic potential $\phi(r)$ is connected with the volume fractions of polymer $\Phi(r)$ and with the concentration of counterions $n(r)$ through the Poisson equation

$$\frac{e}{kT} a^2 \nabla^2 \phi(r) = -\tau \cdot (f\Phi(r) - n(r)b^3) \quad (2)$$

where ϵ is the dielectric constant of the medium and

$$\tau = \frac{4\pi e^2}{\epsilon k T a}$$

is the characteristic dimensionless parameter associated with electrostatic interactions. (In ref.¹³⁾ the analogous parameter is designated as κ .) Large values of τ correspond to solvents of relatively low polarity; for very polar solvents, such as water, at room tem-

perature $\tau \approx 5 - 10$ depending on the value of a . Further calculations are performed for $\tau = 4, 12$ and 25 ; therefore, it will be possible to see the tendency of the change of the results with the variation of solvent polarity.

Within the framework of the self-consistent field approximation the distribution of counterions $n(r)$ obeys the Boltzmann law

$$n(r) = n_0 \cdot \exp(e\varphi(r)/(kT)) \quad (2a)$$

where n_0 is the counterion concentration at the point for which $\varphi(r) = 0$. The Boltzmann law results from the minimum condition of the free energy (1) with respect to $n(r)$ and hence it will not be considered as additional condition in the further calculations.

In the expression (1) for the free energy the first three terms are connected with the translational entropy of polymer chains, molecules of low-molecular-weight solvent and counterions, respectively. The contributions related to the translational entropy of molecules of low-molecular-weight solvent and, especially, of counterions (the second and third terms in the expression (1)) play an important role in the calculations. Note that the corresponding terms were taken into account in refs.¹²⁻¹⁴⁾ in an approximate way only (see below). The fourth term describes the non-Coulomb polymer-solvent interaction. The next term corresponds to the entropy loss, resulting from an inhomogeneous distribution of the polymer volume fraction (the Lifshitz entropy^{28,29)}. To avoid misunderstanding it is worth-while to emphasize that this term is a non-linear expression^{28,29)}; it is not identical to the square gradient term of the linear response theory. The last term together with Eq. (2) describes the electrostatic interactions in the system. If the function $\Phi(r)$ only slightly deviates from the homogeneous distribution, this electrostatic contribution to the free energy can be reduced to the Debye-Hückel expression (cf. ref.¹⁶⁾). However, the Debye-Hückel approximation is sufficient only for the calculation of spinodals; to be able to consider the final microdomain structure and to derive the phase diagram, the full Poisson-Boltzmann equation (see Eqs. (2) and (2a)) should be solved (cf. ref.¹⁸⁾).

Expression (1) together with (2) completely define the free energy of the polyelectrolyte solution having a given spatially inhomogeneous distribution of the local potential $\varphi(r)$ and concentrations $\Phi(r)$ and $n(r)$. Minimizing the expression with respect to the functions $\Phi(r)$ and $n(r)$ we obtain the value of the free energy of the system under consideration in the mean field approximation (MFA). Thereby the equilibrium structure of the system is defined by the symmetry of the functions $\Phi(r)$ and $n(r)$ corresponding to the minimum of the free energy. Even though it is quite possible (see refs.^{13,17)}) to allow for the fluctuation corrections to the free energy (see ref.²²⁾), the MFA calculation is the necessary first step of the theory. Therefore, we restrict ourselves in the present paper to MFA treatment.

To determine the equilibrium structure of the system we assume that the deviations

$$\tilde{\Phi}(r) = \Phi(r) - \langle \Phi \rangle \quad \tilde{n}(r) = n(r) - \langle n \rangle$$

of the functions $\Phi(r)$ and $n(r)$ (and hence $\varphi(r)$) from the average values $\langle \Phi \rangle$ and $\langle n \rangle = f\langle \Phi \rangle/b^3$ are small ($|\tilde{\Phi}(r)| \ll \langle \Phi \rangle$, $|\tilde{n}(r)| \ll \langle n \rangle$). To simplify the notations let us denote $p(r) \equiv n(r)b^3$, $\langle p \rangle = b^3\langle n \rangle$ and

$$\tilde{p}(r) = \tilde{n}(r)b^3 = p(r) - \langle p \rangle$$

with $|\tilde{p}(r)| \ll \langle p \rangle$.

We can expand the free energy (1) into a power series of $\tilde{\Phi}(r)$ and $\tilde{p}(r)$ up to the fourth-order terms

$$\begin{aligned} \frac{F}{kT} = & \frac{F_0}{kT} + \frac{1}{b^3} \int d^3 r \left\{ \frac{1}{2} \left[\frac{\tilde{\Phi}^2}{1 - \langle \Phi \rangle} - 2\chi\tilde{\Phi}^2 + \frac{a^2}{12} \frac{(\nabla \tilde{\Phi})^2}{\langle \Phi \rangle} + \frac{\tilde{p}^2}{\langle p \rangle} \right. \right. \\ & \left. \left. + \frac{e}{kT} \tilde{\varphi} \cdot (f\tilde{\Phi} - \tilde{p}) \right] + \frac{1}{6} \left[\frac{\tilde{\Phi}^3}{(1 - \langle \Phi \rangle)^2} - \frac{a^2}{4} \frac{\tilde{\Phi} \cdot (\nabla \tilde{\Phi})^2}{\langle \Phi \rangle^2} - \frac{\tilde{p}^3}{\langle p \rangle^2} \right] \right. \\ & \left. + \frac{1}{24} \left[\frac{2\tilde{\Phi}^4}{(1 - \langle \Phi \rangle)^3} + \frac{a^2}{\langle \Phi \rangle^3} \tilde{\Phi}^2 \cdot (\nabla \tilde{\Phi})^2 + 2 \frac{\tilde{p}^4}{\langle p \rangle^3} \right] \right\} \end{aligned} \quad (3)$$

where $\frac{F_0}{kT}$ is the value of $\frac{F}{kT}$ for $\Phi(r) = \langle \Phi \rangle$, $p(r) = \langle p \rangle$:

$$\frac{F_0}{kT} = \frac{V}{b^3} \left\{ \frac{\langle \Phi \rangle}{N} \ln \langle \Phi \rangle + (1 - \langle \Phi \rangle) \ln (1 - \langle \Phi \rangle) + \langle p \rangle \ln \langle p \rangle + \chi \langle \Phi \rangle (1 - \langle \Phi \rangle) \right\}$$

V is the volume of the system.

In this notation Eq. (2) takes the form:

$$\frac{e}{kT} a^2 \nabla^2 \tilde{\varphi} = -\tau \cdot (f\tilde{\Phi} - \tilde{p}) \quad (4)$$

By performing the Fourier transformations of the functions $g(r) \equiv \tilde{\Phi}(r), \tilde{p}(r), \tilde{\varphi}(r)$ as follows

$$g(q) = \int e^{iqr} g(r) d^3 r$$

Eq. (4) can be reduced to

$$\frac{e}{kT} a^2 q^2 \tilde{\varphi}(q) = \tau \cdot (f\tilde{\Phi}(q) - \tilde{p}(q)) \quad (5)$$

and expression (3) for the free energy can be rewritten in the following form up to the fourth-order terms (cf. refs.^{3, 17)}):

$$\frac{F}{kT} = \frac{F_0}{kT} + \frac{1}{b^3} \sum_{n=2}^4 \frac{1}{n!} (\Gamma^{(n)} \tilde{\Phi}^{(n)}) \quad (6)$$

$$(\Gamma^{(n)} \tilde{\Phi}^{(n)}) = \sum_{a_1 \dots a_n} \int \Gamma_{a_1 \dots a_n}^{(n)} (q_1 \dots q_n) \prod_{i=1}^n \tilde{\Phi}_{a_i}(q_i) \frac{d^3 q_i}{(2\pi)^3}$$

$$\Gamma_{a_1 \dots a_n}^{(n)} (q_1 \dots q_n) = (2\pi)^3 \tilde{\Gamma}_{a_1 \dots a_n}^{(n)} (q_1 \dots q_n) \delta \left(\sum_{i=1}^n q_i \right)$$

$$\text{with } \tilde{\Phi}_1(q_i) = \tilde{\Phi}(q_i) \quad \tilde{\Phi}_2(q_i) = \tilde{p}(q_i)$$

$$\begin{aligned}\tilde{\Gamma}_{11}^{(2)}(\mathbf{q}) &= \frac{1}{(1 - \langle \Phi \rangle)} - 2\chi + \frac{a^2 q^2}{12 \langle \Phi \rangle} + \frac{\tau f^2}{a^2 q^2} \\ \tilde{\Gamma}_{12}^{(2)}(\mathbf{q}) = \tilde{\Gamma}_{21}^{(2)}(\mathbf{q}) &= - \frac{\tau f}{a^2 q^2} \quad (7)\end{aligned}$$

$$\begin{aligned}\tilde{\Gamma}_{22}^{(2)}(\mathbf{q}) &= \frac{1}{\langle p \rangle} + \frac{\tau}{a^2 q^2} \\ \tilde{\Gamma}_{111}^{(3)}(\mathbf{q}_1, \mathbf{q}_2, \mathbf{q}_3) &= \frac{1}{(1 - \langle \Phi \rangle)^2} - \frac{a^2 \cdot (q_1^2 + q_2^2 + q_3^2)}{24 \langle \Phi \rangle^2} \\ \tilde{\Gamma}_{222}^{(3)}(\mathbf{q}_1, \mathbf{q}_2, \mathbf{q}_3) &= - \frac{1}{\langle p \rangle^2} \quad (8) \\ \tilde{\Gamma}_{1111}^{(4)}(\mathbf{q}_1, \mathbf{q}_2, \mathbf{q}_3, \mathbf{q}_4) &= \frac{2}{(1 - \langle \Phi \rangle)^3} + \frac{a^2}{12 \langle \Phi \rangle^3} (q_1^2 + q_2^2 + q_3^2 + q_4^2) \\ \tilde{\Gamma}_{2222}^{(4)}(\mathbf{q}_1, \mathbf{q}_2, \mathbf{q}_3, \mathbf{q}_4) &= \frac{2}{\langle p \rangle^3}\end{aligned}$$

The wave vector dependencies of the third and forth vertex functions $\tilde{\Gamma}^{(3)}$ and $\tilde{\Gamma}^{(4)}$ are calculated here by expansion of the non-linear Lifshitz entropy expression (fifth term in the integrand of Eq. (1)). Another derivation of the expression for the entropy loss resulting from an inhomogeneous distribution of the polymer volume fraction (in the form of the expansion in powers of the polymer concentration fluctuations up to the fourth order) was presented by one of the authors and Dobrynin in ref.¹⁷⁾ using a rigorous density functional description very similar to the one presented by Leibler in ref.³⁾ for the problem of microphase separation in diblock copolymers.

It can be checked by direct comparison of these two expressions that they give the same wavevector dependencies of the vertices $\tilde{\Gamma}^{(2)}$, $\tilde{\Gamma}^{(3)}$ and $\tilde{\Gamma}^{(4)}$ in the limit $x = q^2 a^2 N / 6 \gg 1$, which is another way to prove the validity of the Lifshitz approximation for this limit. Only the case $x \gg 1$ is important for us for the following reasons:

First, as it can be seen from the final results, the microphase separation studied here corresponds just to those microstructures for which the condition $x \gg 1$ is valid (as a matter of fact, the period of these supercrystal phases turns out to be independent of the degree of polymerisation N ; see below).

Second, even in the region $x \ll 1$ the corrections to our approximation are not essential, because in this case the contribution from the fifth term in Eq. (1) is anyway much smaller than the contributions of the translational entropy of counterions and solvent molecules (see ref.¹⁶⁾).

Note that the first terms in the expressions for $\tilde{\Gamma}_{11}^{(2)}$, $\tilde{\Gamma}_{111}^{(3)}$ and $\tilde{\Gamma}_{1111}^{(4)}$ describe the contributions of the corresponding order due to the translational entropy of the molecules of low-molecular-weight solvent while the first terms in the formulas for $\tilde{\Gamma}_{22}^{(2)}$, $\tilde{\Gamma}_{222}^{(3)}$ and $\tilde{\Gamma}_{2222}^{(4)}$ are due to the translational entropy of counterions. It is very

important to take these terms into account in a proper way. For instance, allowing for these terms in the second-order terms enabled to describe the Debye-Hückel screening in refs.¹³⁻¹⁵. As regards the corresponding third-order terms, their presence leads to a critical point. It is the neglect of these contributions in the third-order terms that led the authors of ref.¹³ to the erroneous conclusion that there exists no critical point in the system under consideration.

To analyze the stability of the homogeneous state of the solution we need to investigate the matrix $\mathbf{G}^{-1} = \parallel \tilde{\Gamma}_{ij}^{(2)}(\mathbf{q}) \parallel$. When the matrix \mathbf{G}^{-1} is a positive definite matrix, the homogeneous state of the system is stable. Hence for definition of the spinodal equation we should determine the eigenvalues of matrix \mathbf{G}^{-1} . Let us denote the maximum eigenvalue as $\lambda_+(\mathbf{q})$ and the minimum eigenvalue (which is of primary importance for our analysis) as $\lambda_-(\mathbf{q})$. The spinodal equation for microparticle separation can be found from the conditions (cf. refs.^{3, 4, 17}):

$$\begin{aligned} \lambda_-(\mathbf{q}) &= 0 \\ \frac{d\lambda_-(\mathbf{q})}{d\mathbf{q}} &= 0 \end{aligned} \tag{9}$$

Eq. (9) determines the critical value of the Flory-Huggins parameter, χ_{cr} , at which the spinodal decomposition via microparticle separation takes place, and the critical wavevector q^* defining the period of the emerging microdomain structure (cf. refs.^{13, 14}):

$$a^2 q^{*2} = f \sqrt{12 \tau \langle \Phi \rangle} - \tau f \langle \Phi \rangle \tag{10}$$

$$\chi_{cr} = \frac{1}{2} \left(\frac{1}{1 - \langle \Phi \rangle} + \frac{\tau f}{\sqrt{3 \langle \Phi \rangle \tau}} - \frac{\tau f}{12} \right) \tag{11}$$

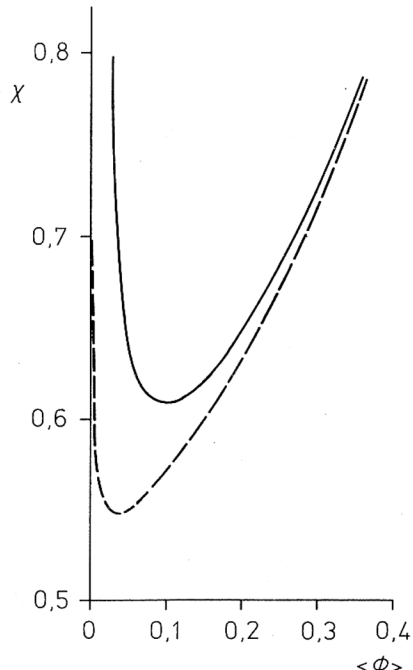


Fig. 1. Spinodal curves for a solution of weakly charged polyelectrolytes ($\tau = 4$; $N = 10^3$; $f = 0,01$). The dotted line is the spinodal for microparticle separation, the solid line is the one for macrophase separation

In Fig. 1 the spinodal curves for macrophase (solid line) and microphase (dotted lines) separation are shown for $\tau = 4$, $N = 10^3$, $f = 0.01$. In the area above the solid curve spinodal decomposition into macroparticles takes place; the area below both curves is the stability region of the disordered phase; between the solid and dotted lines spinodal decomposition goes with the formation of a microdomain structure.

The period D of microdomain structure is given by $D = \frac{2\pi}{q^*}$. It can be seen from Eqs. (10) and (11) that the value of q^* and, thus, D depends on $\langle \Phi \rangle$ and is independent of χ . In Figs. 2–4 we show the dependence of q^* and D on the average volume fraction

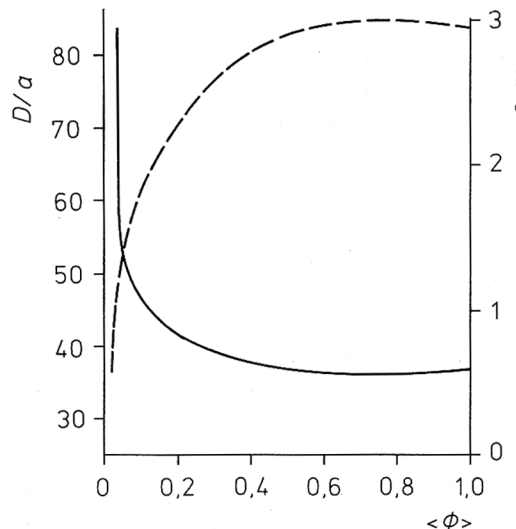


Fig. 2.

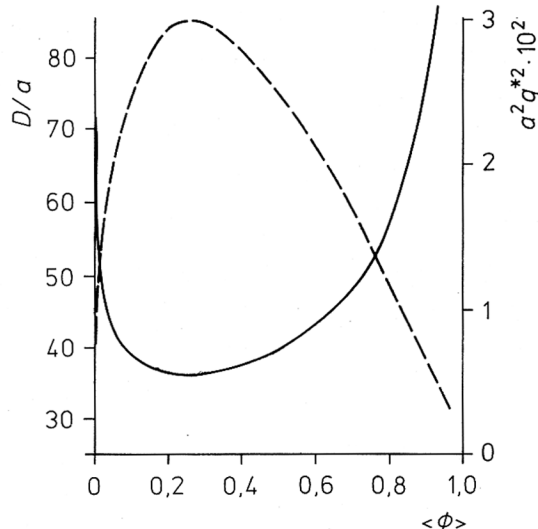


Fig. 3.

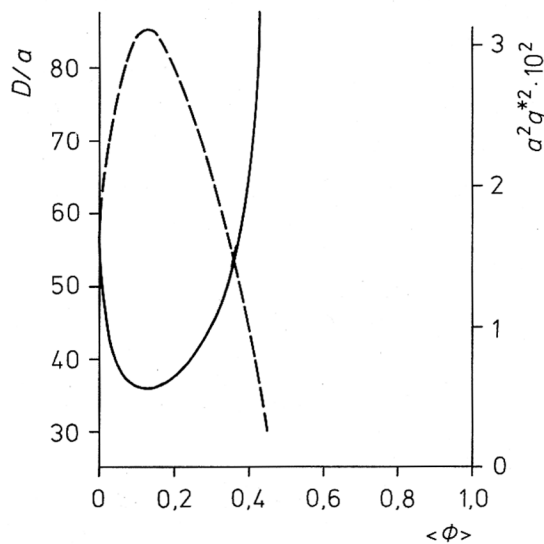


Fig. 4.

Fig. 2. The plots of the period of microstructure D (—) and of the critical wave vector q^* (---) as functions of the average value of volume fraction of polymer $\langle \Phi \rangle$ for the case $\tau = 4$

Fig. 3. The plots of the period of microstructure D (—) and of the critical wave vector q^* (---) as functions of $\langle \Phi \rangle$ for $\tau = 12$

Fig. 4. The plots of the period of microstructure D (—) and of the critical wave vector q^* (---) as functions of $\langle \Phi \rangle$ for $\tau = 25$

of polymer for different values of τ (i.e., for different dielectric constants of the medium, ϵ). As it can be seen from Figs. 2–4 the value of D/a for the case of a solution of polyelectrolytes appears to be numerically large: $D/a \approx 40 - 80$ which corresponds to several hundreds of Å. Thus, the microdomain structures in the present case can be detected with the conventional X-ray and neutron scattering techniques.

Free energies of different microdomain structures

In order to investigate in detail different microdomain structures as well as the transitions between them, we will analyze the higher-order terms of the expansion (6).

Now, when we know the eigenvalues (λ_- , λ_+) and eigenvectors (ψ_1 , ψ_2) of the inverse matrix of correlation functions \mathbf{G}^{-1} , we can represent the expression for the free energy (6) in another form. Let us pass to the basis of eigenvectors ψ_1 , ψ_2 . (Since the matrix \mathbf{G}^{-1} is a symmetrical matrix, its eigenvectors form an orthonormal basis.) In the basis of eigenvectors ψ_1 , ψ_2 the matrix $\mathbf{G}^{-1}(q)$ has a diagonal form, i.e.

$$\mathbf{G}^{-1}\psi_1 = \lambda_-\psi_1, \quad \mathbf{G}^{-1}\psi_2 = \lambda_+\psi_2$$

Let us introduce new variables $U_1(q)$, $U_2(q)$, which diagonalize the quadratic term of the free energy (6)

$$\begin{aligned} (\Gamma^{(2)} \tilde{\Phi}^{(2)}) &= \sum_{i,j} \int \tilde{\Gamma}_{ij}^{(2)}(q) \tilde{\Phi}_i(q) \tilde{\Phi}_j(-q) \frac{d^3 q}{(2\pi)^3} \\ &= \int (\lambda_-(q) U_1(q) U_1(-q) + \lambda_+(q) U_2(q) U_2(-q)) \frac{d^3 q}{(2\pi)^3} \end{aligned} \quad (12)$$

where the variables $\tilde{\Phi}_1(q)$, $\tilde{\Phi}_2(-q)$ are connected with new ones $U_1(q)$, $U_2(q)$ through the equations

$$\tilde{\Phi}_i(q) = \sum_{j=1}^2 C_{ij} \cdot U_j(q) \quad (13)$$

$$C_{11} = D_1/(1 + D_1^2)^{1/2} \quad C_{12} = D_2/(1 + D_2^2)$$

$$C_{21} = 1/(1 + D_1^2)^{1/2} \quad C_{22} = 1/(1 + D_2^2) \quad (14)$$

$$D_1 = -\frac{\tilde{\Gamma}_{12}^{(2)}}{\tilde{\Gamma}_{11}^{(2)} - \lambda_-} \quad D_2 = -\frac{\tilde{\Gamma}_{12}^{(2)}}{\tilde{\Gamma}_{11}^{(2)} - \lambda_+}$$

where $\tilde{\Gamma}_{ij}^{(2)}$ are the elements of the matrix $\mathbf{G}^{-1}(q)$.

The higher-order terms of the free energy (6) in the vicinity of the spinodal curve take the following form

$$\begin{aligned} &\frac{1}{3!} \sum_{a_1 \dots a_3} \tilde{\Gamma}_{a_1 \dots a_3}^{(3)}(q^*) \sum_{q_1 + q_2 + q_3} \tilde{\Phi}_{a_1}(q_1) \tilde{\Phi}_{a_2}(q_2) \tilde{\Phi}_{a_3}(q_3) \\ &+ \frac{1}{4!} \sum_{a_1 \dots a_4} \tilde{\Gamma}_{a_1 \dots a_4}^{(4)}(q^*) \sum_{q_1 + q_2 + q_3 + q_4} \tilde{\Phi}_{a_1}(q_1) \tilde{\Phi}_{a_2}(q_2) \tilde{\Phi}_{a_3}(q_3) \tilde{\Phi}_{a_4}(q_4) \end{aligned} \quad (15)$$

where the values $\tilde{\Gamma}_{a_1 \dots a_n}^{(n)}(\mathbf{q})$ are determined by Eqs. (8). (Near the spinodal the higher-order terms in $\tilde{\Phi}_{a_i}(\mathbf{q}_i)$ have no singularity, so the important fluctuations should be those having the wavevectors $|\mathbf{q}| = q^*$)³⁾. Using Eqs. (13)–(15) we can obtain the expression for the higher-order terms as a function of U_1 and U_2 .

So, we have the expression for the full free energy as a function of two variables U_1 and U_2 . For the description of phase transitions an order parameter is usually introduced¹⁷⁾ which is a variable (or combination of variables) fluctuating most strongly near the point of phase transition. In the present case the role of the order parameter can be played by the fluctuating variable U_1 , associated with the eigenvalue $\lambda_-(q^*) < 0$. In this work, following the method of calculation of refs.^{13, 17)}, we will neglect the influence of weakly fluctuating variables.

The final expression for the expansion of the free energy in powers of the order parameter U_1 up to the fourth term can be written as follows

$$\begin{aligned} \frac{F}{kT} = & \frac{F_0}{kT} + \frac{1}{2} \lambda_- \sum_{\mathbf{q}} U_1(\mathbf{q}) U_1(-\mathbf{q}) + \frac{1}{6} S_3 \sum_{\mathbf{q}_1 + \mathbf{q}_2 + \mathbf{q}_3} U_1(\mathbf{q}_1) U_1(\mathbf{q}_2) U_1(\mathbf{q}_3) \\ & + \frac{1}{24} S_4 \sum_{\mathbf{q}_1 + \mathbf{q}_2 + \mathbf{q}_3 + \mathbf{q}_4} U_1(\mathbf{q}_1) U_1(\mathbf{q}_2) U_1(\mathbf{q}_3) U_1(\mathbf{q}_4) \\ S_3 = & \tilde{\Gamma}_{111}^{(3)}(q^*) C_{11}^3 + \tilde{\Gamma}_{222}^{(3)}(q^*) C_{21}^3 \\ S_4 = & \frac{1}{24} [\tilde{\Gamma}_{1111}^{(4)}(q^*) C_{11}^4 + \tilde{\Gamma}_{2222}^{(4)}(q^*) C_{12}^4] \end{aligned} \quad (16)$$

where C_{ij} are defined by Eqs. (14).

It is worth-while to emphasize once more that it is the translational entropy of low-molecular-weight solvent and counterions that led to several new terms in the expression for the third-order vertex S_3 and to the possibility of cancelling of all these terms at the critical point.

The functional (16) differs from the expression obtained by Leibler for the free energy of diblock-copolymers (cf. ref.³⁾) by the notation only (and, of course, by the physical meaning). Thus, to study the polyelectrolyte system under investigation we can formally use the results of ref.³⁾ Let us rewrite the expression for the free energy (16) as follows

$$\frac{F}{kT} = \frac{F_0}{kT} + \lambda_- \cdot U_n^2 + \alpha_n \cdot U_n^3 + \beta_n \cdot U_n^4 \quad (17)$$

where U_n is the equilibrium value of the amplitude of the order parameter and α_n, β_n are coefficients which depend on the type of the lattice (cf. ref.³⁾):

$$\begin{aligned}
 \text{for a lamellar lattice} \quad \alpha_1 &= 0 & \beta_1 &= \frac{1}{4} S_4 \\
 \text{for a triangular lattice} \quad \alpha_3 &= \frac{2}{3 \cdot 3^{1/2}} S_3 & \beta_3 &= \frac{5}{12} S_4 \\
 \text{for a body-centered-cubic lattice} \quad \alpha_6 &= \frac{4}{3 \cdot 6^{1/2}} S_3 & \beta_6 &= \frac{5}{8} S_4
 \end{aligned} \tag{18}$$

Minimizing the free energy (16) with respect to U_n we obtain the expressions for the free energy of different microdomain structures:

The free energy for a lamellar structure takes the form:

$$\frac{F_1}{kT} = \frac{F_0}{kT} - \frac{\lambda_-^2}{4\beta_1} \tag{19}$$

For the triangular ($n = 3$) and body-centered cubic (bcc) structures ($n = 6$) the free energy is equal to (cf. ref.³)

$$\frac{F_n}{kT} = \frac{F_0}{kT} + \frac{27 \alpha_n^4}{64^2 \beta_n^3} (1 + \gamma_n)^3 (1 - 3 \gamma_n) \tag{20}$$

with

$$\gamma_n = \left(1 - \frac{32 \beta_n \cdot \lambda_-}{9 \alpha_n^2} \right)^{1/2} \tag{21}$$

Phase diagram for a weakly charged polyelectrolyte solved in a poor solvent

In this section we construct the full phase diagram for weakly charged polyelectrolyte solutions and discuss some specific features of it. To this end it is convenient to plot the phase diagram resulting from the quantitative comparison of the free energies of different phases: the disordered phase (Eq. (4)), the lamellar microphase (Eq. (20)), and triangular and bcc microphases (Eq. (21)). This phase diagram (Fig. 5) contains the regions where each of these phases has the lowest free energy. As it can be seen, this phase diagram is qualitatively similar to the phase diagram of diblock-copolymers of ref.³

To construct the full phase diagram one should take into account the possibility of macroscopic phase separation (which is impossible for monodisperse block copolymers). To this end let us consider the chemical potential $\mu = (dF/dN)_{V,T}$ and the pressure $p = -(dF/dV)_{N,T}$ for each phase. From the conditions of phase equilibrium it should be

$$p_1 = p_2 \quad \mu_1 = \mu_2$$

For each pair of coexisting phases the areas of stability of various microphases were found, and the biphasic regions corresponding to the coexistence of two different phases (i.e. the regions of macrophase separation) were determined. The main results

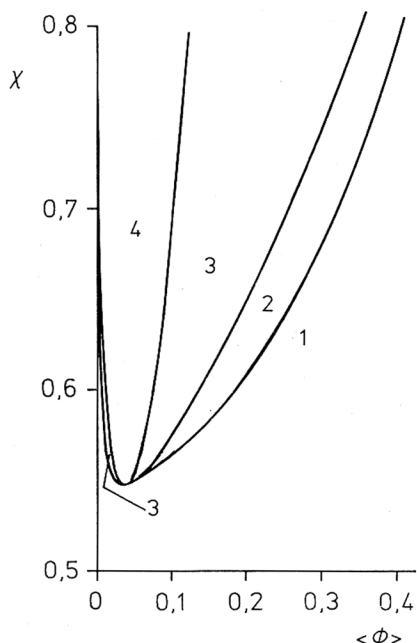


Fig. 5. Phase diagram for the solution of weakly charged polyelectrolytes ($\tau = 4$; $N = 10^3$; $f = 0.01$). The phase diagram shows the regions, where each of the phases has the lowest free energy: the region of disordered phase (1), body-centered-cubic microdomain phase (2), triangular microdomain phase (3) and lamellar microdomain phase (4). The region of low concentrated bcc phase is too narrow to be seen at this scale

of this analysis are shown in the complete phase diagrams (Figs. 6–8). All phase diagrams (including Fig. 5) are plotted in the variables (χ, Φ) for the following values of parameters: $N = 10^3$; $f = 0.01$; $a = b$. In Fig. 6 the phase diagram of a weakly charged polyelectrolyte solution for the case $\tau = 4$ (very polar solvent) is shown. The phase diagram contains the following regions: the region of homogeneous phase (1), the region of bcc structure (2), the region of triangular structure (3), the region of lamellar structure (4) and the region of phase separation (5). The region of bcc phase for the case of low values of Φ is so small that it can not be seen at the scale of the diagram. From the diagram of Fig. 6 it is possible to notice that a considerable part of the diagram is occupied by the regions of phase separation. For relatively large values of χ only the triangular microphase survives, and there are also wide biphasic regions corresponding to the coexistence of triangular and homogeneous phases.

Two other diagrams are plotted for $\tau = 12$ (Fig. 7) and $\tau = 25$ (Fig. 8). These cases correspond to lower polarity of the solvent. The form of the phase diagram of Figs. 7 and 8 is similar to that of Fig. 6. The main quantitative difference is connected with the fact that at large values of τ the regions of stability of microdomain structures become relatively small and the phase separation appears for larger values of χ .

It is worth-while to compare the full phase diagrams obtained in the present paper with the diagrams obtained in other papers^{12, 13, 17}. As it has been mentioned above, in contrast to refs.^{12, 13} in the present paper we properly take into consideration in the expansion for the free energy the contributions connected with translational entropy of molecules of low-molecular-weight solvent and counterions. Also, for the description of the behaviour of the system we use two independent variables Φ and p , which enables us to obtain a more consistent expansion of the free energy in terms of the order parameter. As a result, not only the regions of stability of microphases themselves, but also the biphasic regions are derived from our calculations.

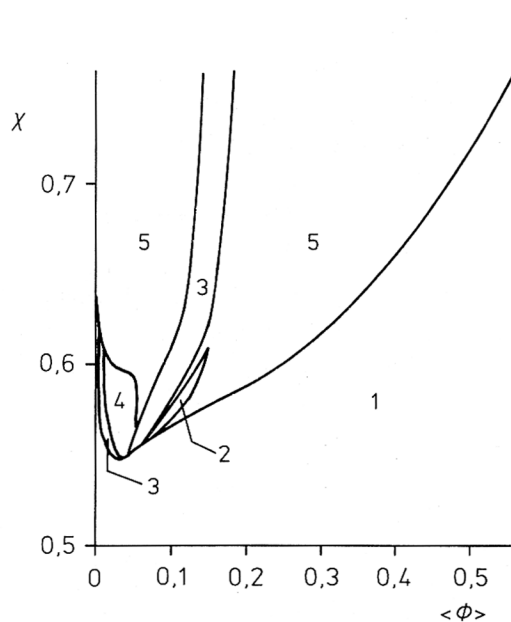


Fig. 6.

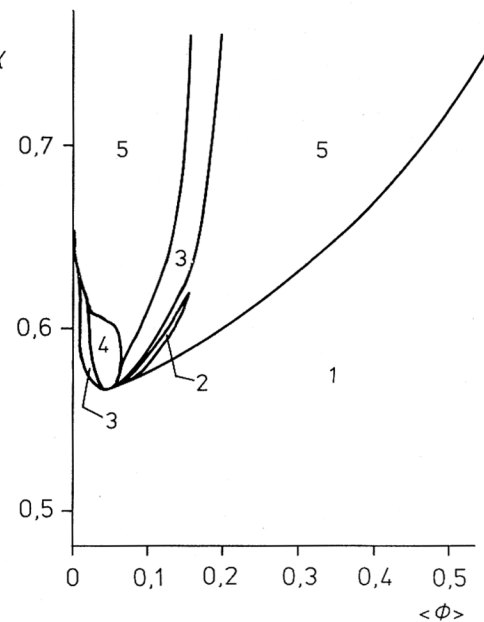


Fig. 7.

Fig. 6. Phase diagram for the solution of weakly charged polyelectrolytes, for $\tau = 4$. The phase diagram contains the following regions: disordered phase (1), body-centered-cubic microdomain phase (2), triangular microdomain phase (3), lamellar microdomain phase region (4) and the regions of phase separation (5)

Fig. 7. Phase diagram for the solution of weakly charged polyelectrolytes, for $\tau = 12$. The notation of the regions is the same as in Fig. 6

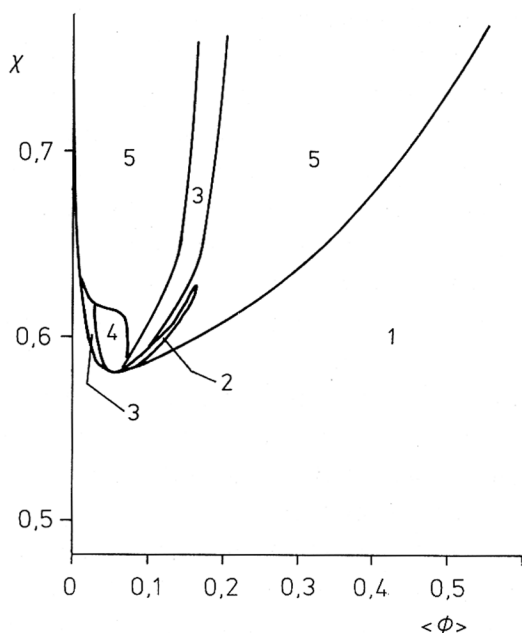


Fig. 8. Phase diagram for the solution of weakly charged polyelectrolytes, for $\tau = 25$. The notation of the regions is the same as in Fig. 6

In ref.¹⁷⁾ the phase diagram for a similar system, viz. a mixture of two polyelectrolytes (weakly charged polyelectrolyte A and uncharged polyelectrolyte B), is obtained. This phase diagram and the diagram obtained in the present paper have similar features; in particular, in both cases for large values of χ wide regions of separation into homogeneous and microdomain phase appear. For the case of polyelectrolyte mixtures¹⁷⁾, however, the microphase surviving at large values of χ is of lamellar type, while for the present case it is of triangular type.

The existence of wide biphasic separation regions for the poor solvent solutions of weakly charged polyelectrolytes permits to formulate the following strategy for the search of microdomain structures: it is worth-while to concentrate on the detailed study of biphasic equilibria. There is a good chance that in this case one of the coexisting phases is in fact microheterogeneous, i. e. it has microdomain structure.

This paper deals with the investigation of solutions of weakly charged polyelectrolytes in the weak segregation approximation and, thus, our results are valid only near the critical point. However from the phase diagrams (Figs. 6–8) it is possible to notice that the regions of stability of different microphases correspond to the parts of the phase diagrams near the critical point, with the exception of the triangular phase region, which spreads also far from the critical point. As for block-copolymers, to obtain the full phase diagram for the present system it is necessary to study additionally the behavior of solutions of weakly charged polyelectrolytes in the strong segregation regime. The results will be described in another publication³⁰⁾.

Finally, the shortcomings of the present approach connected with the mean field character of our calculations should be discussed. It is well known that the mean field approximation is generally poor at low concentrations, and especially near the critical point of the phase diagram where the fluctuations should be taken into account. For the block-copolymer critical point this was done in ref.²²⁾ The methods of accounting for fluctuations in polyelectrolyte systems were discussed in the papers of one of the authors of the present article^{13, 17)}.

However, as it was already emphasized above, the mean field calculation of the phase diagram is a natural first step of the theory. Microphase separation in polyelectrolyte systems was up to now studied much less than for block-copolymers, and even the phase diagram in the mean field approximation was not yet reported in the literature.

On the other hand, this is an actual topic of experimental research. First observation of microdomains in poor solvent polyelectrolyte systems were made in refs.^{25–27)}, and now there is a general need to understand the rough features of the phase diagram. The most important of these rough features that are found in the present study are the following: (i) the existence of wide biphasic regions (regions 5 in Figs. 6–8); (ii) the existence of “islands” of stable microdomain phase *within* phase separation regions (regions 2–4 in Figs. 6–8); (iii) coupling between micro- and macro-phase separation (i. e. microdomain structure appears in one of the coexisting phases *after* macroscopic phase separation). These features definitely do not depend on the fact whether the fluctuations are taken into account.

At the same time, some more refined features of the phase diagram depend on this fact, e. g. the regions of stability of the microphases of different symmetry will be redistributed. However, we feel that it is the understanding of the rough features of the

phase diagram that is now most important for experimental research in this field. This justifies the use of the mean field approximation in the present study.

- ¹⁾ "Developments in Block Copolymers", I. Goodman, Ed., Applied Science, New York 1982 (vol. 1), 1985 (vol. 2)
- ²⁾ E. Helfand, *Macromolecules* **8**, 552 (1975)
- ³⁾ L. Leibler, *Macromolecules* **13**, 1602 (1980)
- ⁴⁾ I. Ya. Erukhimovich, *Vysokomol. Soedin., Ser. A*: **24**, 1942 (1982); *Polym. Sci. USSR* **24**, 2223 (1983)
- ⁵⁾ A. N. Semenov, *Sov. Phys.-JETP (Engl. Transl.)* **61**, 733 (1985)
- ⁶⁾ E. I. Shakhnovich, A. M. Gutin, *J. Phys. (Paris)* **50**, 1843 (1989)
- ⁷⁾ S. V. Panukov, S. I. Kuchanov, *Zh. Eksp. Teor. Fiz.* **99**, 659 (1991)
- ⁸⁾ A. V. Dobrynin, I. Ya. Erukhimovich, *JETP Lett. (Engl. Transl.)* **53**, 570 (1991)
- ⁹⁾ G. H. Fredrickson, S. T. Millner, *Phys. Rev. Lett.* **67**, 835 (1991)
- ¹⁰⁾ K. Binder, H. Frisch, *J. Chem. Phys.* **81**, 2126 (1984)
- ¹¹⁾ H. Frisch, A. Yu. Grosberg, *Makromol. Chem., Theory Simul.* **2**, 517 (1993)
- ¹²⁾ V. Yu. Borue, I. Ya. Erukhimovich, *Sov. Phys.-Dokl. (Engl. Transl.)* **31**, 146 (1986)
- ¹³⁾ V. Yu. Borue, I. Ya. Erukhimovich, *Macromolecules* **21**, 3240 (1988)
- ¹⁴⁾ J. F. Joanny, L. Leibler, *J. Phys. (Paris)* **51**, 545 (1990)
- ¹⁵⁾ I. A. Nyrkova, A. R. Khokhlov, E. Yu. Kramarenko, *Vysokomol. Soedin., Ser. A*: **32**, 918 (1990); *Polym. Sci. USSR* **32**, 852 (1990)
- ¹⁶⁾ A. R. Khokhlov, I. A. Nyrkova, *Macromolecules* **25**, 1493 (1992)
- ¹⁷⁾ A. V. Dobrynin, I. Ya. Erukhimovich, *Zh. Eksp. Teor. Fiz.* **99**, 1344 (1991); *Sov. Phys.-JETP (Engl. Transl.)* **72**, 751 (1991)
- ¹⁸⁾ I. A. Nyrkova, M. Doi, A. R. Khokhlov, *Polym. Prepr. (Am. Chem. Soc. Div. Polym. Chem.)* **34 (1)**, 926 (1993)
- ¹⁹⁾ I. A. Nyrkova, A. R. Khokhlov, M. Doi, *Macromolecules* **26**, 3601 (1993)
- ²⁰⁾ A. R. Khokhlov, I. Ya. Erukhimovich, *Macromolecules* **26**, 7195 (1993)
- ²¹⁾ V. V. Vasilevskaya, S. G. Starodubtzev, A. R. Khokhlov, *Vysokomol. Soedin, Ser. B*: **29**, 390 (1987)
- ²²⁾ G. H. Fredrickson, E. Helfand, *J. Chem. Phys.* **87**, 697 (1987)
- ²³⁾ E. Helfand, Z. R. Wasserman, *Macromolecules* **9**, 879 (1976); **11**, 960 (1978); **13**, 994 (1980)
- ²⁴⁾ A. N. Semenov, *Macromolecules* **22**, 2849 (1989)
- ²⁵⁾ F. Schlosseler, A. Moussaid, J. P. Munch, S. J. Candau, *J. Phys. II (Paris)* **1**, 1197 (1991)
- ²⁶⁾ A. Moussaid, F. Schlosseler, J. P. Munch, S. J. Candau, *J. Phys. II (Paris)* **3**, 573 (1993)
- ²⁷⁾ M. Shibayama, T. Tanaka, C. Han, *J. Chem. Phys.* **97**, 6842 (1992)
- ²⁸⁾ A. Yu. Grosberg, A. R. Khokhlov, "Statistical Physics of Macromolecules", Nauka Publishers, Moscow 1989
- ²⁹⁾ I. M. Lifshitz, A. Yu. Grosberg, A. R. Khokhlov, *Rev. Mod. Phys.* **50**, 683 (1978)
- ³⁰⁾ I. A. Nyrkova, M. Doi, A. R. Khokhlov, to be published